



# Structural characterisation of nucleoside loaded low density lipoprotein as a main criterion for the applicability as drug delivery system

Michal Hammel, Peter Laggner, Ruth Prassl\*

*Institute of Biophysics and X-Ray Structure Research, Austrian Academy of Sciences, Schmiedlstrasse 6, A-8042 Graz, Austria*

Received 24 June 2002; received in revised form 11 December 2002; accepted 13 December 2002

## Abstract

The potential role of human low density lipoprotein (LDL) particles as delivery system for lipophilic, cytotoxic drugs critically depends on their structural integrity. In the present study, LDL particles were loaded with antineoplastic prodrugs, i.e. monooleoyl (MOT)- and dioleoyl (DOT)- thymidine esters by different techniques. Using the reconstitution method MOT shows the highest incorporation efficiency with over 80% of the initial drug associated with LDL. In contrast, for the more lipophilic DOT the incorporation efficiency for reconstitution, dry film as well as dimethylsulfoxide method was extremely low. Structural changes upon drug loading were monitored by differential scanning calorimetry (DSC) and small angle X-ray scattering (SAXS). The results show that the influence of MOT and DOT is predominantly confined to the surface monolayer of LDL seen as a destabilisation of the protein moiety and a small increase in particle diameter. The core lipid region of the LDL-drug complexes remains essentially unaffected, as verified by undisturbed core lipid arrangement and core lipid melting behaviour.

© 2003 Elsevier Science Ireland Ltd. All rights reserved.

**Keywords:** Low density lipoprotein (LDL); Drug carrier; Differential scanning calorimetry (DSC); Small angle X-ray scattering (SAXS); LDL reconstitution; Thymidine derivatives

## 1. Introduction

A number of systems such as microspheres (Okada and Toguchi, 1995), liposomes (Allen et al., 1995; Lasic, 1996) and other macromolecules (Duncan, 1992) have been proposed as targeting carriers to deliver cytotoxic drugs. Obstacles to the

successful delivery of drugs using these carrier moieties are their rapid uptake by the reticulo-endothelial system, instability of the carrier drug conjugates and defective targeting to non-targeted cells like liver cells. In order to overcome these shortcomings new drug delivery systems need to be developed.

Human plasma low density lipoproteins (LDLs) are water-soluble nanoparticles which may be regarded as natural counterparts of liposomes. Physiologically, LDL serves as the primary trans-

\* Corresponding author. Tel.: +43-316-4120-305; fax: +43-316-4120-390.

E-mail address: [ruth.prassl@oeaw.ac.at](mailto:ruth.prassl@oeaw.ac.at) (R. Prassl).

port vehicle of cholesterol and water-insoluble natural compounds, such as vitamins and hormones to various cell types (Esterbauer et al., 1992). The obvious idea to exploit this lipophilic carrier properties in the aqueous environment of blood for the purpose of drug delivery has been early recognised (Krieger et al., 1979; Gal et al., 1981), but so far the successful application for therapeutic purposes is still lacking. The apolar lipid core of LDL, which attains a fluid, oily consistence at physiological temperatures is best qualified to act as an efficient lipophilic solubilising medium. The second site for drug intercalation is the phospholipid surface monolayer, however, close to the surface the drugs are less well protected from hydrolysis (Firestone, 1994) and drugs may undergo spontaneous exchange (redistribution) with other lipoprotein subspecies in plasma (de Smidt et al., 1992).

The rationale to use LDL as delivery system for cytotoxic compounds, however, lies in the fact that tumour tissues display elevated receptor-mediated uptake of LDL as compared with normal tissues (Ho et al., 1978; Gal et al., 1981; Hynds et al., 1984; Norata et al., 1984; Vitols et al., 1992). This overexpression of LDL receptors can be explained by a high cholesterol demand for cell growth or by mechanisms directly linked to cell transformation (Favre, 1992). Various methods for the incorporation of antineoplastic lipophilic drugs into LDL were reported and some of the resultant drug-LDL complexes proved to be cytotoxic towards tumour cells *in vitro* via the LDL receptor dependent pathway (Samadi-Baboli et al., 1989, 1990; de Smidt and van Berkel, 1990; Lestavel-Delattre et al., 1992; Samadi-Baboli et al., 1993; de Smidt et al., 1993). However, little is known about the impact of drug incorporation on the structural integrity of the particle, which is an important factor in controlling rates of metabolic processes, as receptor binding or enzyme activity. For the use of liposomes, it has turned out that size heterogeneity, phospholipid composition, degree of saturation and chain length as well as the nature of the phospholipid headgroup strongly influence the suitability of the liposomal formulation as delivery system (Treat et al., 2001; Hong et al., 2001). Although for LDL the chemical composition

(Chapman et al., 1988; Kostner and Laggner, 1989) and the molecular arrangement of lipid and protein is predetermined (Orlova et al., 1999; Hevonoja et al., 2000), it will be indispensable to investigate, if drug incorporation induces structural changes. Hence, a physico-chemical characterisation, i.e. determination of different parameters like phospholipid-shell and cholesteryl-ester-core morphology, conformation of apolipoprotein B-100 (apoB-100) and aggregation tendency are important to assess the applicability of the LDL-drug complex as a delivery system. In the present study the integrity of the LDL-drug complexes is investigated by small angle X-ray scattering (SAXS) yielding information about particle size, aggregation behaviour and the organisation of the lipid core (Laggner et al., 1976, 1977; Laggner and Müller, 1978; Müller et al., 1978; Luzzati et al., 1979; Baumstark et al., 1990). Further, the core lipid melting behaviour is monitored by differential scanning calorimetry (DSC) (Deckelbaum et al., 1977; Schuster et al., 1995; Pregetter et al., 1999) and conformational changes of apoB-100 are deduced from the thermal unfolding behaviour of the protein (Prassl et al., 1998), yielding information about modifications of the protein induced by drug incorporation.

As a first step we decided not to use highly cytotoxic drugs but non-toxic model systems. We have focused on pyrimidine derivatives, as representative compounds for antimetabolites (Schultis et al., 1991) used either as anticancer drugs (5-fluorodeoxyuridine) or for antiviral therapy like human immunodeficiency virus (HIV) infection, based on the inhibition of reverse transcriptase (Azidothymidine, Stavidine).

## 2. Materials and methods

### 2.1. Materials

Thymidine (purity >99%), oleoyl chloride (purity tech ~70%) and dry pyridine (max. 0.0075% H<sub>2</sub>O, purity >95%) were supplied by Fluka (Vienna, Austria). Thin layer chromatography (TLC) plates (silica 60 preformed layers on aluminium sheets) and preparative TLC plates

(silica 60 preformed 0.25 mm thick layers on glass plates) were obtained from Merck (Darmstadt, Germany). All other chemicals and solvents were of analytical grade obtained from Sigma (Vienna, Austria).

## 2.2. Synthesis of 3',5'-dioleoyl thymidine (DOT)

The procedure as described by Nishizawa and Casida (1965), modified by Bijsterbosch et al. (1994), utilising oleoyl chloride was followed to convert thymidine to DOT (Fig. 1). Briefly, to 100 mg of thymidine (0.4 mmol) dissolved in 8 ml of dry dimethylacetamide (DMAC) 1.7 ml of dry pyridine and 0.8 ml of oleoyl chloride (2 mmol) were added. After incubation for 24 h at 65 °C, the reaction mixture was transferred to a separa-

tory funnel containing 100 ml H<sub>2</sub>O and 50 ml CHCl<sub>3</sub>. The organic phase was washed once with 100 ml of 10% (w/v) NaHCO<sub>3</sub> and twice with 100 ml H<sub>2</sub>O, and subsequently the organic solvent was evaporated. The resulting yellowish oil showed two spots upon analysis by TLC and UV detection at 254 nm (solvent:methanol/dichlormethan 5:95), a major spot with  $R_f = 0.67$  and a minor spot with  $R_f = 0.13$ . Thymidine, pyridine and oleoyl chloride markers are detected with  $R_f < 0.05$ ,  $R_f \sim 0.45$  and  $R_f > 0.95$ , respectively. By analogy to the TLC analysis of 3',5'-dioleoyl-5-iodo-2'-deoxyuridine shown by Bijsterbosch et al. (1994) we have attributed the major spot to DOT and the minor spot to 5'-monooleoyl thymidine, the hydrolysis product of DOT. The two products were separated by preparative TLC performed at similar condi-

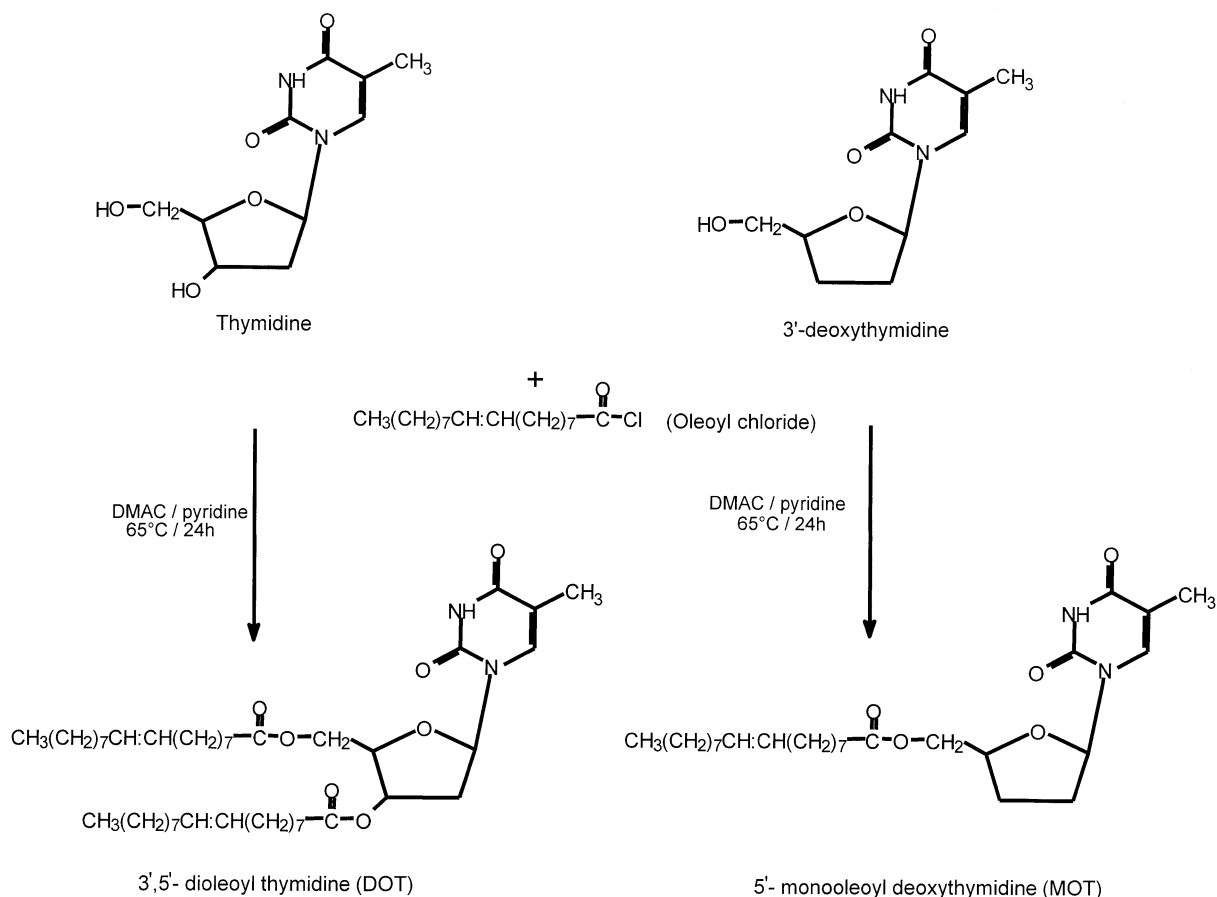


Fig. 1. Synthesis of DOT and MOT.

tions as the analytical TLC. The purified DOT (transparent oily substance) was stored at  $-20\text{ }^{\circ}\text{C}$ . The final purity of DOT was analysed by HPLC (Beckman Gold System) using a reversed-phase  $7\text{ }\mu\text{m}$  LiChrosorb RP-18 column ( $4 \times 250\text{ mm}$ ) from Merck. Fifty microlitre aliquots of DOT dissolved in the mobile phase (Acetonitril:THF, 80:20 v/v) were eluted at a flow rate of 1.0 ml/min and monitored by UV detection (Beckman Gold System) at 270 nm. The typical HPLC retention time for DOT was  $R_t = 11.0\text{ min}$ . A minor peak ( $\sim 15\%$  of the major peak) with a retention time of  $R_t = 8.7\text{ min}$  was identified as 5'-monooleoyl thymidine. This impurity could not be removed by further purification using preparative chromatography, which suggests hydrolysis of DOT during the HPLC assay.

### 2.3. Synthesis of 5'-monooleoyl deoxythymidine (MOT)

An identical procedure as described for DOT was used to convert 3'-deoxythymidine to MOT (Fig. 1). The resulting white solid product showed one single spot upon analysis by TLC with  $R_f = 0.38$ . The purity of MOT was confirmed by HPLC assay as described for DOT. The typical HPLC retention time for MOT was  $R_t = 3.3\text{ min}$ .

### 2.4. Plasma and LDL preparation

Plasma was prepared as described by Kleinvelde et al. (1992). Briefly, blood was drawn from normolipidemic donors after overnight-fasting and the EDTA-plasma was separated immediately by low spin centrifugation at  $4\text{ }^{\circ}\text{C}$ . A sucrose solution (final concentration 0.6%) was added and aliquots were stored at  $-80\text{ }^{\circ}\text{C}$  in the dark. LDL was obtained by ultracentrifugation using a single step discontinuous gradient in a Beckman NVT 65 rotor at 60 000 rpm ( $342\,000 \times g$  at  $r_{\text{max}} = 84.9\text{ mm}$ ) for 2h at  $10\text{ }^{\circ}\text{C}$  as described (Ramos et al., 1995). LDL was filtered through a  $0.2\text{ }\mu\text{m}$  syringe filter into sterile vials and stored at  $4\text{ }^{\circ}\text{C}$  under argon in the dark up to 7 days.

### 2.5. Preparation of drug-LDL complexes

Three different incorporation methods were used for DOT, whereas for MOT just the reconstitution method was applied.

#### 2.5.1. Reconstitution method

In principle, the drugs were incorporated into LDL as described by Masquelier et al. (1986). The key step in this procedure is the lyophilisation of LDL in presence of sucrose as protecting agent. Briefly, 4–6 mg LDL were transferred into a glass tube containing 10 mg sucrose per mg LDL (40% sucrose solution). LDL mass was calculated from the protein concentration as determined by BCA-assay (see below) taken as 22% weight fraction from total mass. The solution was rapidly frozen at  $-80\text{ }^{\circ}\text{C}$  and lyophilised over night. Subsequently, a solution of MOT in diethyl ether in a concentration range of 0.005–0.1 mg MOT per 1 mg LDL corresponding to approximately 30–530 MOT molecules per LDL particle was added to the dry LDL extract. DOT dissolved in diethyl ether was added in a concentration range of 0.01–0.25 mg DOT per 1 mg LDL corresponding to approximately 30–840 DOT molecules per LDL particle. The organic solvent was evaporated by a stream of  $\text{N}_2$  followed by vacuum evaporation for at least 4 h. The LDL complex was reconstituted by addition of 300  $\mu\text{l}$  of 10 mM phosphate buffered saline (PBS), pH 7.2 per mg LDL by gentle shaking over night at  $4\text{ }^{\circ}\text{C}$ . As a control, LDL without drug was treated in the same manner, referred to as reconstituted control LDL.

#### 2.5.2. Dry film method

One millilitre DOT (1 mg/ml, 1.29 mM) dissolved in dichlormethan was coated on the surface of a glass-tube by evaporation of organic solvent in a stream of  $\text{N}_2$  followed by drying in vacuum for at least 4 h. Then 3 ml LDL (approximately 2.5 mg/ml LDL) in PBS containing 270  $\mu\text{M}$  EDTA and 83 mg/ml gentamycin were added. The final concentration of DOT was 0.2 mg per mg LDL that corresponds to approximately 680 DOT molecules per LDL particle. The mixture was incubated for 24 h at  $37\text{ }^{\circ}\text{C}$  under argon in the dark, while gently shaking (Kader et al., 1998;

Tauchi et al., 2000). LDL without drug was incubated at the same conditions as a control.

### 2.5.3. Dimethylsulfoxide (DMSO) method

Small aliquots (40  $\mu$ l) of concentrated stock solution of DOT in DMSO (50 mM, 38.5 mg/ml) were added to 3 ml LDL solution (approximately 2.5 mg/ml LDL in PBS containing 0.01% EDTA) resulting in a final DMSO concentration of 1.3% (v/v) and 0.2 mg DOT per mg LDL, which corresponds to approximately 680 DOT molecules per LDL particle. The solution was incubated for 3 h at 20 °C under argon in the dark, covered with an aluminium foil, while gently shaking in an orbital shaker (de Smidt et al., 1993; Pussinen et al., 2000). As a control experiment LDL was incubated with DMSO at the same conditions. As reported by de Smidt et al. (1993) up to 5% DMSO do not modify native LDL as assessed by agarose gel electrophoresis and density ultracentrifugation.

Further treatment of the LDL-drug complexes was similar for all three incorporation methods. The unbound drugs were separated by a single step ultracentrifugation in a TL 120 tabletop ultracentrifuge (350 000  $\times g$  at  $r_{av}$ ) using a TLA-100.4 rotor (Beckman, Austria) (Schumaker and Puppione, 1986; Pussinen et al., 2000). Briefly, 3.3 ml PBS (pH 7.4; containing 270  $\mu$ M EDTA and 83 mg/ml gentamycin,  $d=1.006$  g/ml) were underlayered with 1.7 ml of density-adjusted LDL-complex ( $d=1.24$  g/ml, adjusted by addition of 381 mg solid KBr/ml LDL-complex) and spun at 100 000 rpm for 2 h at 10 °C. By this way, the LDL-complexes float and the free amphiphilic thymidine derivatives are pelleted (Schultis et al., 1991). Finally, the samples were passed through a corning disposable syringe filter (0.45  $\mu$ m) in order to remove huge aggregates of LDL.

Irrespective of the incorporation technique the LDL-drug complexes were dialysed against PBS before measurements.

### 2.6. Compositional analysis of LDL samples

Total cholesterol was determined with the CHOD-PAP enzymatic test kit (Roche Diagnostics GmbH, Vienna, Austria). Free cholesterol was

determined with the Free Cholesterol C-test (Wako Chemicals GmbH, Neuss, Germany). Cholesteryl ester (CE) content was calculated as (total cholesterol–freecholesterol)  $\times 1.7$ . This factor takes into account the average molecular weight ratio of CE to free cholesterol. Phospholipids and triglycerides were assayed by two enzymatic test kits (bioMérieux, France). Protein was measured by the bicinchoninic acid assay (BCA assay, Pierce, The Netherlands).

### 2.7. HPLC assay

The concentration of drugs in the complexes was measured by HPLC as follows: 50  $\mu$ l of LDL samples were extracted by 4 ml dichlormethane. The organic fraction was centrifuged for 10 min at 5000  $\times g$  in glass vials. A part of the organic fraction was evaporated under N<sub>2</sub>. The residual was dissolved in 0.5 ml of mobile phase (acetonitril:THF, 80:20 v/v) and 50  $\mu$ l aliquots were injected in a HPLC system (Beckman Gold System) using reversed-phase 7  $\mu$ m LiChrosorb RP-18 columns (4  $\times$  250 mm, Merck) with a flow rate of 1.0 ml/min. The eluate was monitored by UV detection at 270 nm. The concentrations were determined with respect to a standard curve of the drug.

### 2.8. Differential scanning calorimetry (DSC)

DSC was performed on a high-sensitivity, adiabatic differential scanning microcalorimeter Microcal VP-DSC (MicroCal Inc., Northampton, MA). Samples were concentrated using Centricon 10 concentrators (Millipore, Vienna, Austria) to a final concentration of 1–2 mg/ml protein. The filtrate was used to fill the reference cell and for detection of the buffer baseline. The thermograms of LDL were recorded in a temperature range of 5–90 °C at a heating rate of 1 °C/min. For data acquisition and analysis the ORIGIN 5.0 software package provided by MicroCal Inc. was used. Briefly, after subtraction of the buffer baseline, the raw data were normalised to heat capacity units taking into account the heating rate, the volume of the cell and the molecular mass. These thermograms were interpreted in terms of melting transi-

tion temperatures ( $T_m$ ) and calorimetric enthalpies ( $\Delta H_{\text{cal}}$ ).  $T_m$  was taken as the temperature corresponding to the thermal midpoint of the transition.  $\Delta H_{\text{cal}}$  of the core lipid melting transition was obtained after baseline adjustment, and equals the area under the curve. In the case of the core melting transition the  $\Delta H_{\text{cal}}$  values obtained in kilocalories per mole (kcal/mol) were recalculated to Joule per gram (J/g) using a mean molecular mass of 650 for CE. For the unfolding of apo-B100 it was impossible to calculate precise enthalpic values, as the exothermic denaturation transition hampers baseline setting.

### 2.9. Small-angle X-ray scattering (SAXS)

SAXS was measured with an integrated small angle X-ray camera system (HECUS-MBraun, Graz, Austria), based on the Kratky line collimator, equipped with an one-dimensional position sensitive detector, a Ni-filtered beam-stop system, and an automatic temperature and data collection unit. The camera was attached to a rotating anode generator (RU-200B; Rigaku Denki, Japan) operating at 2 kW power. Samples were concentrated using Centricon 10 concentrators (Millipore) to a final concentration of 7 mg/ml protein. SAXS measurements of the samples filled in 1 mm quartz capillaries were performed at 20 °C with an exposure time of 1 h. Even for long exposure times (8 h) no aggregation of native LDL was found. The scattering curves were monitored in the scattering vector range  $q$  from 0.08 to 2.6/nm ( $q = 4\pi \sin \theta/\lambda$ ), with  $2\theta$  being the scattering angle with respect to the incident beam and  $\lambda = 0.1542$  nm (Cu-K $\alpha$  radiation) being the wavelength of the X-rays. The scattering curves were normalised to the relative integral primary beam intensity and the buffer baseline was subtracted. The principle of desmearing and Inverse Fourier Transform of the data convoluted with the slit collimated beam profile were applied as described previously (Müller et al., 1978). In particular, the program GIFT (Bergmann et al., 2000) was used to calculate the electron pair distance distribution functions. The real space  $p(r)$  function contains information about the internal electron density distribution, and the spatial distance distribution and hence

about the overall particle shape. The maximum particle diameter  $D_{\text{max}}$  is defined as the distance  $r_{\text{max}}$  where  $p(r)$  approaches zero. The determination of the exact value of  $r_{\text{max}}$  was difficult due to the poorly defined intercept with the abscissa towards larger distances, which is a consequence of the low accuracy of the  $I(q)$  values at very low angles ( $q < 0.2/\text{nm}$ ). Therefore, the maximum in the  $p(r)$  function which is located around  $r = 20$  nm and corresponds to the electron density auto-correlation of the outer phospholipid headgroups and the protein moiety, was used as indication for changes in particle size upon drug loading.

## 3. Results

### 3.1. Chemical analysis

For native LDL the proportions of total cholesterol (CHOL), triglyceride (TG) and phospholipid (PL) to apo-B100 were found to be in good agreement with data reported in literature (Westesen et al., 1995). Both control and drug-loaded LDL showed no significant differences in the lipid composition as compared with native LDL (see Table 1). The amount of incorporated drug was determined by HPLC and is also given in Table 1. For the reconstitution procedure the low incorporation efficiency for DOT (<1%) in comparison to MOT (up to 80%) was obvious, hence two additional procedures, i.e. the dry film and the DMSO method were tried to improve the incorporation efficiency for DOT. With the dry film method no improvement in DOT incorporation (DOT/LDL =  $2 \pm 1$  mol/mol) was achieved, whereas with DOT dissolved in DMSO a slight improvement, namely DOT/LDL =  $12 \pm 5$  mol/mol was obtained. However, the incorporation efficiency of DOT was still less than 2% from the initial amount of drug. Besides, almost the double amount of the hydrolysis product of DOT was found to be incorporated in LDL. Worth mentioning, that the non-incorporated drug was associated with the aggregates, which were removed by centrifugation and filtration before (see Section 2).

It has to be stated, that the DMSO method could not be tested for MOT, as MOT is insoluble

Table 1  
Chemical composition of native, control and drug loaded LDL samples

Sample	Concentration ratios <sup>a,b</sup>			Initial amount of drug (mol of drug/mol of LDL) <sup>c</sup>	Incorporated amount of drug (mol of drug/mol of LDL) <sup>a,c</sup>
	CHOL	TG	PL		
LDL native	1.95±0.15	0.77±0.06	0.21±0.02	–	–
<i>Reconstitution method</i>					
LDL-control	1.96±0.19	0.72±0.05	0.18±0.06	–	–
LDL-MOT	1.63	0.73	0.04	530	153
	1.88	0.74	0.14	265	99
	1.70	0.64	0.15	53	38
	1.78			27	22
LDL-DOT	1.86	0.75	0.27	840	2
	1.80	0.70	0.30	590	3
	1.85	0.64	0.15	340	2
	1.96			170	2
	1.83			34	1
<i>Dry film method</i>					
LDL-control	1.81±0.10	0.76±0.17	0.18±0.01	–	–
LDL-DOT	1.77	0.80	0.21	680	2±1
<i>DMSO method</i>					
LDL-control	2.12	0.83	0.17	–	–
LDL-DOT	2.06	0.81	0.15	680	12±5

<sup>a</sup> Data are expressed as means ( $n=2$ ) or means±S.D. ( $n=3$ ).

<sup>b</sup> Concentration (mg/ml) ratios of cholesterol (CHOL), triglycerides (TG) and phospholipids (PL) to protein.

<sup>c</sup> A molecular weight of 491 for MOT, 771 for DOT and 2 500 000 for LDL has been used to calculate the molar ratio of drug to LDL.

in DMSO. However, due to the high incorporation efficiency obtained for MOT by the reconstitution method it seemed not necessary to aim at further improvements.

### 3.2. Differential scanning calorimetry (DSC)

In general, upon heating from 5 to 80 °C two endothermic transitions are observed for LDL. The first transition with a  $T_m$  value at ~30 °C corresponds to the order-disorder transition of the core lipids ('core-lipid melting') (Deckelbaum et al., 1975, 1977). The second transition with a  $T_m$  at approximately 80 °C corresponds to the unfolding of apoB-100 (Deckelbaum et al., 1975; Walsh and Atkinson, 1990). At even higher temperatures (85–90 °C) an additional exothermic transition corresponding to particle aggregation was observed. Rescanning of the LDL samples revealed the absence of all transitions (data not shown), which is a clear indication that the thermal induced

aggregation of LDL is irreversible. Representative thermograms for the core-lipid melting are shown in Fig. 2A. The  $T_m$  values for all LDL preparations varied between 29.5 and 30.5 °C (Table 2) and are in good agreement with data published earlier (Prassl et al., 1998). The  $\Delta H_{cal}$  values for the LDL-drug complexes displayed no significant deviations from the values calculated for native LDL ( $\Delta H_{cal} = 2.0 \pm 0.3$  J/g of CE) except a slight decrease in enthalpy for LDL samples loaded by the DMSO method, yielding  $\Delta H_{cal} = 1.4$  J/g of CE and  $\Delta H_{cal} = 1.7$  J/g of CE for control LDL and LDL-DOT complexes, respectively.

The main impact of drugs, however, was observed on the transition temperature of apoB-100 (Table 2) which was decreased for all LDL-drug complexes in comparison to LDL samples without drugs. The values of  $T_m = 78.8 \pm 0.5$  and  $79.8 \pm 0.4$  °C for native and control LDL, respectively, are in keeping with data reported previously (Prassl et al., 1998). The slight increase in  $T_m$

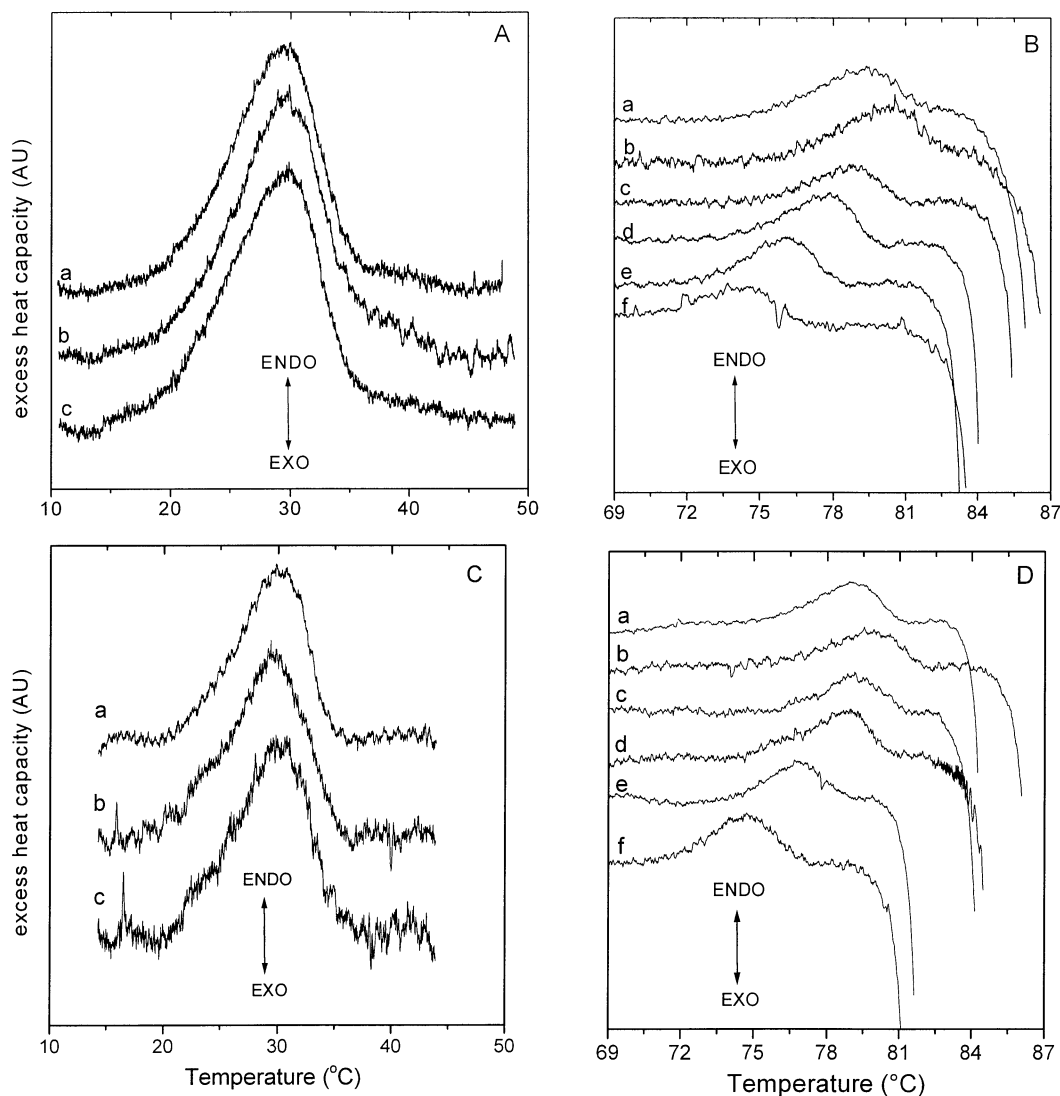


Fig. 2. (A) Excess heat capacity vs. temperature functions of the core lipid melting for native LDL (a), reconstituted control LDL (b) and LDL-DOT complexes prepared by reconstitution method with an initial DOT concentration of 840 mol DOT/mol LDL (c). (B) Excess heat capacity vs. temperature functions of the thermal unfolding of apoB-100 for native LDL (a), reconstituted control LDL (b), and LDL-DOT complexes prepared by reconstitution method with an initial DOT concentration of 34 (c), 170 (d), 340 (e), 840 (f) DOT/LDL mol/mol. (C) Excess heat capacity vs. temperature functions of the core lipid melting for native LDL (a), reconstituted control LDL (b) and LDL-MOT complexes prepared by reconstitution method with an initial MOT concentration of 530 mol MOT/mol LDL (c). (D) Excess heat capacity vs. temperature functions of the thermal unfolding of apoB-100 for native LDL (a), reconstituted control LDL (b), and LDL-MOT complexes prepared by reconstitution method with an initial MOT concentration of 27 (c), 53 (d), 265 (e), 530 (f) MOT/LDL mol/mol.

( $\Delta T_m \sim 1$  °C) for reconstituted control LDL in comparison to native LDL might be an indication that the reconstitution procedure by itself exerts even a stabilising effect on apo-B100, which results

in a more homogeneous particle size distribution (see SAXS results). For the LDL-drug complexes the decrease of  $T_m$  strongly depends on the amount of drug used for incorporation. For the

Table 2  
Calorimetric behaviour of native, control and drug loaded LDL samples

Sample	Core melting <sup>a</sup>		Protein unfolding <sup>a</sup>	Incorporated amount of drug (mol of drug /mol of LDL) <sup>a,c</sup>
	$T_m$ (°C)	$\Delta H_{cal}$ (J/g of CE) <sup>b</sup>	$T_m$ (°C)	
LDL native	29.9±0.05	2.0±0.3	78.8±0.5	–
<i>Reconstitution method</i>				
LDL-control	29.5±0.3	2.2±0.6	79.8±0.4	–
LDL-MOT	29.9	2.3	74.6	153
	29.8	2.0	76.7	99
	29.8	2.6	78.9	38
	29.9	1.8	79.1	22
LDL-DOT	30.0	2.2	73.7	2
	30.3	2.3	76.2	3
	30.5	2.1	77.8	2
	30.3	2.2	78.6	2
<i>Dry film method</i>				
LDL-control	29.9±0.1	2.7±0.6	78.6±0.5	–
LDL-DOT	29.7±0.4	2.7±0.6	73.6±2.4	2±1
<i>DMSO method</i>				
LDL-control	29.9	1.4	78.8	–
LDL-DOT	29.9	1.7	74.1	12±5

<sup>a</sup> Data are expressed as means ( $n = 2$ ) or means ± S.D. ( $n = 3$ ).

<sup>b</sup> A mean molecular weight of 650 was used for cholesterol ester (CE).

<sup>c</sup> A molecular weight of 491 for MOT, 771 for DOT and 2 500 000 for LDL has been used to calculate the molar ratio of drug to LDL.

LDL-MOT samples the maximal decrease of  $\Delta T_m \sim 5$  °C was observed for the highest concentration of MOT, yielding 153 MOT molecules per LDL particle. In contrast, even a low amount of DOT molecules led to a dramatic decrease of the endothermic transition with a maximal shift in  $T_m$  of  $\Delta T_m \sim 6$  °C. Typical thermograms of LDL-drug complexes prepared by the reconstitution method and by incubation with different initial DOT concentrations are shown in Fig. 2B. It can be seen, that in addition to the shift of the endothermic high-temperature transition also the exothermic break in the heating curve, which corresponds to the aggregation of LDL particles, is shifted to lower temperatures. The decrease of the endothermic transition temperature indicates changes in the conformational state of apoB-100 caused by destabilisation of the protein structure, which is also reflected in the lower aggregation temperature of the LDL particles.

Typical thermograms for the unfolding behaviour of apoB-100 in LDL-DOT complexes pre-

pared by either dry film or DMSO procedure are shown in Fig. 3. The  $T_m$  values for the control samples  $T_m = 78.6 \pm 0.5$  and 78.8 °C for dry film and DMSO method, respectively, showed no significant differences in comparison to the native LDL preparation (Table 2), whereas the exothermic aggregation occurred at lower temperatures. This enhanced aggregation tendency might be due to some preformed aggregates of LDL already present in the control sample. For both incorporation methods the DOT treated samples also showed a pronounced shift in the endothermic transition temperature of  $\Delta T_m = 4-5$  °C.

Taken together, our data clearly show that incubation of LDL with both DOT and MOT destabilises apoB-100 with a significant increase in the aggregation tendency of LDL particles.

### 3.3. Small-angle X-ray scattering (SAXS)

Fig. 4A shows the desmeared scattering curves for native, reconstituted control and drug loaded

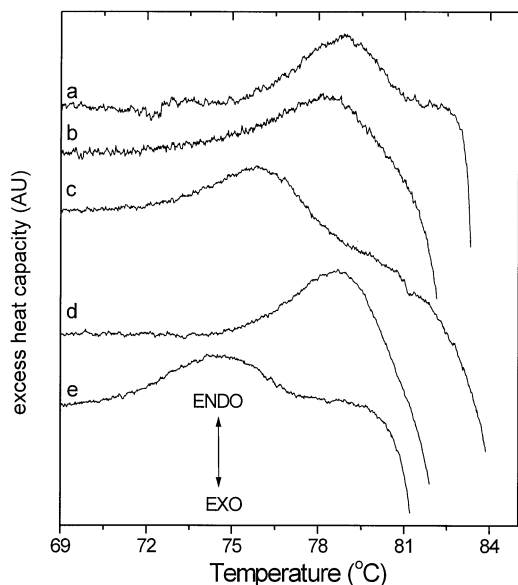


Fig. 3. Representative excess heat capacity vs. temperature functions of the thermal unfolding of apoB-100 for native LDL (a), control LDL (b), LDL-DOT complexes (c) prepared by dry film method and control LDL (d) and LDL-DOT complexes (e) prepared by DMSO method. The heating rate was 1 °C/min. The protein concentration was about 1 mg/ml. The buffer baseline was subtracted and the data were normalised to the protein concentration.

LDL measured at 20 °C. As illustrated, the basic scattering features of LDL obtained by the reconstitution method are very similar to each other at least in regard to the characteristic maximum around  $q = 1.7/\text{nm}$ . However, the lower  $q$ -values for the maximum of the first angular position for LDL-DOT,  $q = 0.32/\text{nm}$  and for LDL-MOT,  $q = 0.33/\text{nm}$  in comparison to control LDL,  $q = 0.34/\text{nm}$  and native LDL,  $q = 0.34/\text{nm}$  indicate a slight increase in mean particle size for drug-loaded LDL. The corresponding electron pair distance distribution functions  $p(r)$  are shown in Fig. 4B. All  $p(r)$  functions exhibit a number of well-pronounced submaxima located at 1.6, 4.3 and 7.6 nm corresponding to the architecture of the lipid core. The submaxima are marked with dotted line arrows. The outer peak at large distances corresponds to the electron density autocorrelation of the phospholipid shell and the

protein. For reconstituted control LDL this peak maximum was located at  $r = 19.7$  nm, whereas for LDL-DOT and LDL-MOT a shift to higher values  $r = 20.3$  and 20.0 nm, respectively, was observed. The differences in the maxima of the  $p(r)$  function between reconstituted control LDL and LDL-DOT samples are marked with solid line arrows. For native LDL measured at the same conditions, the maximum was found at  $r = 20.0$  nm and was slightly broadened in comparison to reconstituted control LDL. As a broad peak is an indication for heterogeneity in particle size, one could deduce that the reconstitution procedure applied for the control sample increases homogeneity, which coincides with our results obtained from DSC. The similarity of the scattering profiles as well as of the  $p(r)$  functions reveal that neither the reconstitution procedure nor drug loading have altered the overall structural features of the LDL particles, however, the shift of the maxima to higher values indicates a slight increase in particle diameter.

Fig. 5A shows typical scattering profiles for LDL samples prepared by the dry film method and measured at the same conditions as mentioned above. Again, the scattering profiles were similar to each other. The pronounced maximum around  $q = 1.7/\text{nm}$  was found at the same angular position for all LDL preparations. However, probably due to long incubation times, i.e. 24 h, a shift of the maximum of the first angular position to smaller angles,  $q = 0.28$  and  $0.30/\text{nm}$  for control LDL and LDL-DOT, respectively, as compared with native LDL,  $q = 0.34/\text{nm}$  was observed indicative of aggregation. The corresponding  $p(r)$  functions are shown in Fig. 5B. No significant changes in the core lipid organisation, characterised by the location of the submaxima at 1.6, 4.3 and 7.6 nm, marked as dotted line arrows, was detected. In contrast, the peak maximum at large distances, marked with a solid line arrow, displayed obvious differences between samples. For native LDL, the peak maximum was determined at  $r = 19.9$  nm. For control LDL, the peak is broadened with a shift of the maximum to a higher value  $r = 20.4 \pm 0.05$  nm (calculated as an average of three independent preparations). Additional broadening and a significant shift to even higher values is

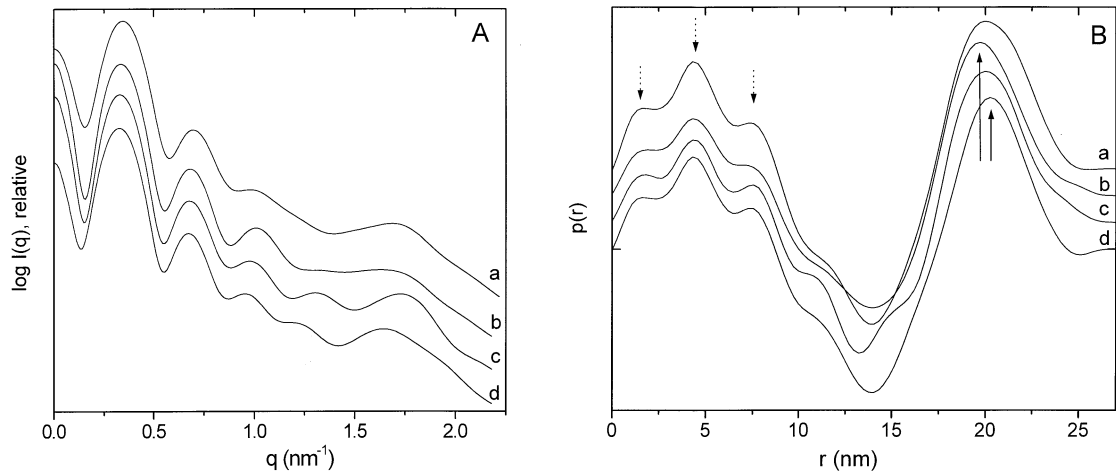


Fig. 4. (A) Desmeared small-angle X-ray scattering curves for native LDL (a), reconstituted control LDL (b), LDL-MOT (c) and LDL-DOT (d) complexes prepared by reconstitution method by incubation with 530 MOT molecules or 840 DOT molecules per LDL molecule, respectively. (B) Electron-pair distance distribution functions  $p(r)$  are shown, corresponding to the scattering curves displayed in (A). In the calculations a maximum fitting dimension  $D_{\max}$  of 27 nm was used. Submaxima at 1.6, 4.3 and 7.6 nm corresponding to the architecture of lipid core are marked with dotted line arrows. The maxima of the peaks for control and LDL-DOT complexes corresponding to the electron density autocorrelation function of the phospholipid headgroups and the protein moiety are marked with solid line arrows. The results are presented in a waterfall graph.

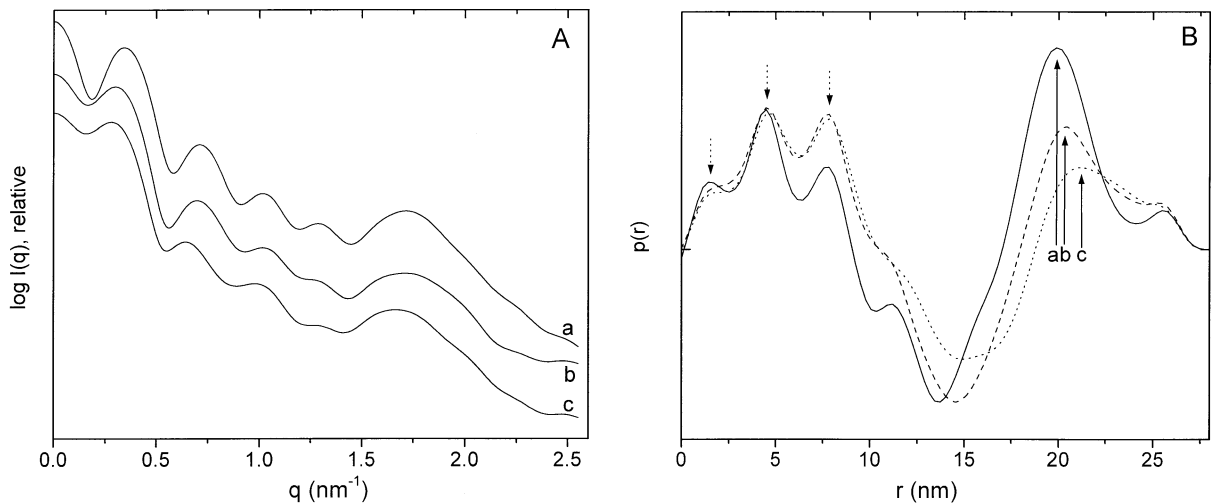


Fig. 5. (A) Desmeared small-angle X-ray scattering curves for native LDL (a), control LDL (b) and LDL-DOT (c) complexes prepared by dry film method. An initial drug concentration of 680 DOT/LDL (mol/mol) was used. (B) Electron-pair distance distribution functions  $p(r)$  are shown, corresponding to the scattering curves displayed in (A). In the present calculations a maximum fitting dimension  $D_{\max}$  of 28 nm was used. Submaxima at 1.6, 4.3 and 7.6 nm corresponding to the architecture of lipid core are marked with dotted line arrows. The maxima of the peaks corresponding to the electron density autocorrelation function of the phospholipid headgroups and protein moiety are marked with solid line arrows.

observed for LDL–DOT samples,  $r = 21.5 \pm 0.4$  nm (calculated as an average of three independent preparations). Note, that this increase in particle size is probably due to the formation of aggregates.

#### 4. Discussion

In the past decade a number of more or less promising attempts to use lipoprotein related particles as a drug carrier for anticancer therapy have appeared in the literature (reviewed by Firestone, 1994; Rensen et al., 2001). An enormous advantage of LDL as compared with liposomal formulations lies in the fact that LDL as natural component of blood induces no immune response. The key notion, however, is the recognised fact that tumour cells in general possess a higher level of LDL receptor activity than normal cells, which facilitates specific binding and internalisation of LDL by cancer cells (Rensen et al., 1997). Another important aspect concerns the prolonged life-time of LDL in circulation as LDL is biodegradable and not recognised by the reticulo-endothelial system. However, one of the main requirements for the successful use of LDL as drug delivery system is that drug-loading does not alter structural properties of LDL, which are essential determinants for receptor recognition. The central task of the current study was to identify structural changes in LDL caused by incorporation of model drugs representative for antimetabolites. Two thymidine derivatives of distinct lipophilicity were synthesised and incorporated in LDL by different techniques. Thymidine was coupled via an ester linkage with one (MOT) or two oleic acids (DOT). Oleoyl residues were chosen as lipophilic anchor as they are abundant components of LDL, whereas the ester linkage ensures release of the original drug at the site of the delivery (Sinkula and Yalkowsky, 1975). Oleic acid was already used by other groups as anchor for hydrophilic compounds like ‘compound 25’ (Krieger et al., 1979), methotrexate, 5-fluorodeoxyuridine (FDU) (de Smidt et al., 1992), eliptinium (Samadi-Baboli et al., 1989, 1990). Thus, our results might be taken

as guideline for the applicability of the LDL complexes to deliver lipophilic compounds.

For DOT three different incorporation techniques were tested for their efficiency, whereas for MOT only the reconstitution procedure was applied. Latter involves the lyophilisation of LDL in the presence of sucrose as protective agent. The drug in organic solution was mixed with the dry extract of LDL, followed by organic solvent evaporation and LDL reconstitution in aqueous buffer (Firestone et al., 1984; Masquelier et al., 1986). We found that the reconstitution method did not alter the chemical composition of LDL, hence we suppose that the organic solvent has not permanently removed lipids from the dry LDL extract prepared in the presence of sucrose. For MOT an incorporation efficiency of 80% of the initial amount of drug with about  $\sim 150$  MOT molecules per LDL particle was achieved by this method, whereas for DOT only negligible amounts of drug were successfully incorporated. These results are consistent with those of a study using the thymidine analogue 5-fluorodeoxyuridine, in which a higher incorporation efficiency ( $> 40\%$ ) was obtained for the monooleoyl derivative in comparison to the dioleoyl derivative ( $< 2\%$ ) (de Smidt et al., 1992). The low incorporation efficiency for DOT could be based on the low water-solubility of DOT, resulting in an extremely low concentration of DOT monomers in the water phase. Besides, DOT was susceptible to hydrolysis, therefore, an even higher amount of the corresponding 5' monooleoyl derivative was found to be trapped in LDL. Only for DOT dissolved in DMSO higher amounts ( $12 \pm 5$  DOT/LDL mol/mol) could be incorporated in LDL. This could be due to a better interaction of LDL with the drug in a suspension in comparison to a drug in solid state. Nevertheless, most of the drug was associated with aggregates as analysed by HPLC, indicating that during incubation DOT caused denaturation of LDL.

One principal finding of the present study was the fact that DSC and SAXS have turned out as adequate and complementary methodologies to monitor structural changes in LDL induced by drug incorporation. For example, changes in the characteristics of the core lipid melting behaviour

as seen by DSC would provide information on the localisation of the drugs in the core and on their influence on the core lipid arrangement. According to our DSC results which are summarised in Table 2 no effect of MOT or DOT on the core lipid melting behaviour of LDL was detected. Hence, these results imply that the drugs are rather located in the phospholipid shell than in the core or at least that the drugs do not influence the melting temperature, which in turn is directly correlated to the chemical composition of the core (Pregetter et al., 1999). The significant differences in the thermotropic unfolding behaviour of apoB-100 for the LDL-drug complexes further point to a surface location of the drug molecules. The shift in  $T_m$  to lower values strongly depends on the amount of MOT and DOT molecules used for incorporation. Even in the case of LDL-DOT preparations with negligible number of incorporated DOT molecules a pronounced shift of  $T_m$  was observed. This could be explained by direct interaction between DOT and apoB-100 during incubation, which influences protein stability and facilitates aggregation of LDL. This behaviour might be based on the strong dipole structure of the DOT molecule, which is caused by the linkage of two hydrophobic oleic acids to the hydrophilic thymidine. Although MOT is less invasive and has a minor dipole than DOT, the high uptake rate of the molecule by LDL is probably responsible for a similar structural destabilisation of the protein moiety.

The integrity of LDL-drug complexes was further investigated by SAXS, yielding information about particle dimensions and core lipid organisation. Earlier SAXS studies have indicated that LDLs are quasi-spherical particles with diameters between 20 and 25 nm, which reveal an internal layered arrangement of lipids below the core melting transition temperature (Laggner et al., 1976, 1977; Laggner and Müller, 1978; Müller et al., 1978; Luzzati et al., 1979; Baumstark et al., 1990). A direct comparison between native LDL and control LDL confirms that the incorporation procedures by itself did not affect the overall structure of the particles. Further, for all LDL-drug preparations the SAXS results confirm our DSC experiments, in a way that no impact of the

drug on the lipid core organisation was observed. For the reconstitution procedure we found no effect on particle size, but a more homogeneous particle size distribution was observed for reconstituted control LDL in comparison to native LDL. This result is in keeping with an electron microscopy study done by Rumsey et al. (1992) in which reconstitution of LDL yields smaller particles with a slightly more homogeneous particle size distribution. The SAXS data are also consistent with DSC data in terms of stabilisation of apoB-100 in reconstituted control LDL.

For drug-loaded LDL prepared by reconstitution method the overall structure was the same, only a slight increase in particle size for LDL-DOT occurred. For the dry film procedure a significant aggregation of the control samples was detected, which indicates the susceptibility of LDL to modifications following a 24 h incubation at 37 °C. There might also be some oxidation of arachidonate phospholipid, which increases surface polarity and electron density of the particle. Accordingly, the increase in particle size can only be attributed to some swelling of the LDL particles.

In conclusion, the present study has shown that it is possible to convert hydrophilic drugs like pyrimidine analogues into lipophilic prodrugs which can be incorporated into LDL. Nevertheless, our data clearly point out that the choice of the lipophilic anchor is an important point for successful application. As the monooleoyl derivative showed a ~100 times higher incorporation efficiency with less effect on the structural features of LDL it seems likely that less hydrophobic prodrugs are more effective. Finally, we could show that the influence of the thymidine esters is predominantly confined to the surface, whereas the lipid core region remains essentially unaffected. The prodrugs used in this study are most probably incorporated in the phospholipid shell where they exert a strong effect on the structure of apo-B100. Our study showed that the structural characterisation of LDL-drug complexes might be an important indicator for further preclinical studies using LDL as drug delivery system.

## Acknowledgements

We thank Dr Manfred Kriechbaum for helpful discussion and Veronika Sattler for excellent technical assistance. This work was supported by a grant from the Austrian Science Foundation (Project P13872-CHE to R.P.).

## References

- Allen, T.M., Newman, M.S., Woodle, M.C., Mayhew, E., Uster, P.S., 1995. Pharmacokinetics and anti-tumor activity of vincristine encapsulated in sterically stabilized liposomes. *Int. J. Cancer* 62, 199–204.
- Baumstark, M.W., Kreutz, W., Berg, A., Frey, I., Keul, J., 1990. Structure of human low-density lipoprotein subfractions, determined by X-ray small-angle scattering. *Biochim. Biophys. Acta* 1037, 48–57.
- Bergmann, A., Fritz, G., Glatter, O., 2000. Solving the generalized indirect Fourier transformation (GIFT) by Boltzmann simplex simulated annealing (BSSA). *J. Appl. Crystallogr.* 33, 1212–1216.
- Bijsterbosch, M.K., Schouten, D., van Berkel, T.J., 1994. Synthesis of the dioleoyl derivative of iododeoxyuridine and its incorporation into reconstituted high density lipoprotein particles. *Biochemistry* 33, 14073–14080.
- Chapman, M.J., Laplaud, P.M., Luc, G., Forgez, P., Bruckert, E., Goulinet, S., Lagrange, D., 1988. Further resolution of the low density lipoprotein spectrum in normal human plasma: physicochemical characteristics of discrete subspecies separated by density gradient ultracentrifugation. *J. Lipid Res.* 29, 442–458.
- de Smidt, P.C., van Berkel, T.J., 1990. LDL-mediated drug targeting. *Crit. Rev. Ther. Drug Carrier Syst.* 7, 99–120.
- de Smidt, P.C., Versluis, A.J., van Berkel, T.J., 1992. Transport of sulfonated tetraphenylporphine by lipoproteins in the hamster. *Biochem. Pharmacol.* 43, 2567–2573.
- de Smidt, P.C., Versluis, A.J., van Berkel, T.J., 1993. Properties of incorporation, redistribution, and integrity of porphyrin—low-density lipoprotein complexes. *Biochemistry* 32, 2916–2922.
- Deckelbaum, R.J., Shipley, G.G., Small, D.M., Lees, R.S., George, P.K., 1975. Thermal transitions in human plasma low density lipoproteins. *Science* 190, 392–394.
- Deckelbaum, R.J., Shipley, G.G., Small, D.M., 1977. Structure and interactions of lipids in human plasma low density lipoproteins. *J. Biol. Chem.* 252, 744–754.
- Duncan, R., 1992. Drug-polymer conjugates: potential for improved chemotherapy. *Anticancer Drugs* 3, 175–210.
- Esterbauer, H., Gebicki, J., Puhl, H., Jürgens, G., 1992. The role of lipid peroxidation and antioxidants in oxidative modification of LDL. *Free Radiol. Biol. Med.* 13, 341–390.
- Favre, G., 1992. Targeting of tumor cells by low density lipoproteins: principle and use of ellipticin derivatives. *C. R. Seances. Soc. Biol. Fil.* 186, 73–87.
- Firestone, R.A., 1994. Low-density lipoprotein as a vehicle for targeting antitumor compounds to cancer cells. *Bioconjug. Chem.* 5, 105–113.
- Firestone, R.A., Pisano, J.M., Falck, J.R., McPhaul, M.M., Krieger, M., 1984. Selective delivery of cytotoxic compounds to cells by the LDL pathway. *J. Med. Chem.* 27, 1037–1043.
- Gal, D., Ohashi, M., MacDonald, P.C., Buchsbaum, H.J., Simpson, E.R., 1981. Low-density lipoprotein as a potential vehicle for chemotherapeutic agents and radionucleotides in the management of gynecologic neoplasms. *Am. J. Obstet. Gynecol.* 139, 877–885.
- Hevonoja, T., Pentikainen, M.O., Hyvonen, M.T., Kovanen, P.T., Ala-Korpela, M., 2000. Structure of low density lipoprotein (LDL) particles: basis for understanding molecular changes in modified LDL [in process citation]. *Biochim. Biophys. Acta* 1488, 189–210.
- Ho, Y.K., Smith, R.G., Brown, M.S., Goldstein, J.L., 1978. Low-density lipoprotein (LDL) receptor activity in human acute myelogenous leukemia cells. *Blood* 52, 1099–1114.
- Hong, M.S., Lim, S.J., Lee, M.K., Kim, Y.B., Kim, C.K., 2001. Prolonged blood circulation of methotrexate by modulation of liposomal composition. *Drug Deliv.* 8, 231–237.
- Hynds, S.A., Welsh, J., Stewart, J.M., Jack, A., Soukop, M., McArdle, C.S., Calman, K.C., Packard, C.J., Shepherd, J., 1984. Low-density lipoprotein metabolism in mice with soft tissue tumours. *Biochim. Biophys. Acta* 795, 589–595.
- Kader, A., Davis, P.J., Kara, M., Liu, H., 1998. Drug targeting using low density lipoprotein (LDL): physicochemical factors affecting drug loading into LDL particles. *J. Control. Release* 55, 231–243.
- Kleinveld, H.A., Hak-Lemmers, H.L.M., Stalenhoef, A.F.H., Demacker, P.N.M., 1992. Improved measurement of low-density lipoprotein susceptibility to copper-induced oxidation: application of a short procedure for isolating low-density lipoprotein. *Clin. Chem.* 38, 2066–2072.
- Kostner, G.M., Laggner, P., 1989. In: *Human Plasma Lipoproteins*. J.C. Fruchart and J. Shepherd, (Eds.), Walter de Gruyter, Berlin, N.Y. Chemical and physical properties of lipoproteins. 23–54.
- Krieger, M., Smith, L.C., Anderson, R.G.W., Goldstein, J.L., Kao, Y.J., Pownall, H.J., Gotto, A.M., Jr, Brown, M.S., 1979. Reconstituted low density lipoprotein: a vehicle for the delivery of hydrophobic fluorescent probes to cells. *J. Supramol. Struct.* 10, 467–478.
- Laggner, P., Müller, K., 1978. The structure of serum lipoproteins as analysed by X-ray small-angle scattering. *Q. Rev. Biophys.* 11, 371–425.
- Laggner, P., Müller, K., Kratky, O., Kostner, G., Holasek, A., 1976. X-ray small angle scattering on human plasma lipoproteins. *J. Colloid Interf. Sci.* 55, 102–108.
- Laggner, P., Degovics, G., Müller, K.W., Glatter, O., Kostner, G.M., Holasek, A., 1977. Molecular packing and fluidity of

- lipids in human serum low density lipoproteins. Hoppe-Seyler's Z. Physiol. Chem. 358, 771–778.
- Lasic, D.D., 1996. Doxorubicin in sterically stabilized liposomes. *Nature* 380, 561–562.
- Lestavel-Delattre, S., Martin-Nizard, F., Clavey, V., Testard, P., Favre, G., Doualin, G., Houssaini, H.S., Bard, J.M., Duriez, P., Delbart, C., 1992. Low-density lipoprotein for delivery of an acrylophenone antineoplastic molecule into malignant cells. *Cancer Res.* 52, 3629–3635.
- Luzzati, V., Tardieu, A., Aggerbeck, L.P., 1979. Structure of serum low-density lipoprotein. *J. Mol. Biol.* 131, 435–473.
- Masquelier, M., Vitols, S., Peterson, C., 1986. Low-density lipoprotein as a carrier of antitumoral drugs: in vivo fate of drug-human low-density lipoprotein complexes in mice. *Cancer Res.* 46, 3842–3847.
- Müller, K., Laggner, P., Glatter, O., Kostner, G.M., 1978. The structure of human-plasma low-density lipoprotein B. *Eur. J. Biochem.* 82, 73–90.
- Nishizawa, Y., Casida, J.E., 1965. 3',5'-Diester of 5-fluoro-2'-deoxyuridine: synthesis and biological activity. *Biochem. Pharmacol.* 14, 1605–1619.
- Norata, G., Canti, G., Ricci, L., Nicolini, A., Trezzi, E., Catapano, A.L., 1984. In vivo assimilation of low density lipoproteins by a fibrosarcoma tumour line in mice. *Cancer Lett.* 25, 203–208.
- Okada, H., Toguchi, H., 1995. Biodegradable microspheres in drug delivery. *Crit. Rev. Ther. Drug Carrier Syst.* 12, 1–99.
- Orlova, E.V., Sherman, M.B., Chiu, W., Mowri, H., Smith, L.C., Gotto, A.M., 1999. Three-dimensional structure of low density lipoproteins by electron cryomicroscopy. *Proc. Natl. Acad. Sci. USA* 96, 8420–8425.
- Prassl, R., Schuster, B., Laggner, P., Flamant, C., Nigon, F., Chapman, M.J., 1998. Thermal stability of apolipoprotein B100 in low-density lipoprotein is disrupted at early stages of oxidation while neutral lipid core organization is conserved. *Biochemistry* 37, 938–944.
- Pregetter, M., Prassl, R., Schuster, B., Kriechbaum, M., Nigon, F., Chapman, J., Laggner, P., 1999. Microphase separation in low density lipoproteins. Evidence for a fluid triglyceride core below the lipid melting transition. *J. Biol. Chem.* 274, 1334–1341.
- Pussinen, P.J., Lindner, H., Glatter, O., Reicher, H., Kostner, G.M., Wintersperger, A., Malle, E., Sattler, W., 2000. Lipoprotein-associated alpha-tocopheryl-succinate inhibits cell growth and induces apoptosis in human MCF-7 and HBL-100 breast cancer cells. *Biochim. Biophys. Acta* 1485, 129–144.
- Ramos, P., Gieseg, S.P., Schuster, B., Esterbauer, H., 1995. Effect of temperature and phase transition on oxidation resistance of low density lipoprotein. *J. Lipid Res.* 36, 2113–2128.
- Rensen, P.C.N., Schiffelers, R.M., Versluis, A.J., Bijsterbosch, M.K., Van Kuijk-Meuwissen, M.E., van Berkel, T.J., 1997. Human recombinant apolipoprotein E-enriched liposomes can mimic low-density lipoproteins as carriers for the site-specific delivery of antitumor agents. *Mol. Pharmacol.* 52, 445–455.
- Rensen, P.C., de Vruhe, R.L., Kuiper, J., Bijsterbosch, M.K., Biessen, E.A., van Berkel, T.J., 2001. Recombinant lipoproteins: lipoprotein-like lipid particles for drug targeting. *Adv. Drug Deliv. Rev.* 47, 251–276.
- Rumsey, S.C., Galeano, N.F., Arad, Y., Deckelbaum, R.J., 1992. Cryopreservation with sucrose maintains normal physical and biological properties of human plasma low density lipoproteins. *J. Lipid Res.* 33, 1551–1561.
- Samadi-Baboli, M., Favre, G., Blancy, E., Soula, G., 1989. Preparation of low density lipoprotein-9-methoxy-ellipticin complex and its cytotoxic effect against L1210 and P 388 leukemic cells in vitro. *Eur. J. Cancer Clin. Oncol.* 25, 233–241.
- Samadi-Baboli, M., Favre, G., Bernadou, J., Berg, D., Soula, G., 1990. Comparative study of the incorporation of ellipticine-esters into low density lipoprotein (LDL) and selective cell uptake of drug-LDL complex via the LDL receptor pathway in vitro. *Biochem. Pharmacol.* 40, 203–212.
- Samadi-Baboli, M., Favre, G., Canal, P., Soula, G., 1993. Low density lipoprotein for cytotoxic drug targeting: improved activity of elliptinium derivative against B16 melanoma in mice. *Br. J. Cancer* 68, 319–326.
- Schultis, H.W., von Baeyer, H., Neitzel, H., Riedel, E., 1991. Preparation of nucleoside-LDL-conjugates for the study of cell-selective internalization: stability characteristics and receptor affinity. *Eur. J. Clin. Chem. Clin. Biochem.* 29, 665–674.
- Schumaker, V.N., Puppione, D.L., 1986. Sequential flotation ultracentrifugation. *Methods Enzymol.* 128, 155–170.
- Schuster, B., Prassl, R., Nigon, F., Chapman, M.J., Laggner, P., 1995. Core lipid structure is a major determinant of the oxidative resistance of low density lipoprotein. *Proc. Natl. Acad. Sci. USA* 92, 2509–2513.
- Sinkula, A.A., Yalkowsky, S.H., 1975. Rationale for design of biologically reversible drug derivatives: prodrugs. *J. Pharm. Sci.* 64, 181–210.
- Tauchi, Y., Zushida, I., Yokota, M., Chono, S., Sato, J., Ito, K., Morimoto, K., 2000. Inhibitory effect of dexamethasone palmitate-low density lipoprotein complex on low density lipoprotein-induced macrophage foam cell formation. *Biol. Pharm. Bull.* 23, 466–471.
- Treat, J., Damjanov, N., Huang, C., Zrada, S., Rahman, A., 2001. Liposomal-encapsulated chemotherapy: preliminary results of a phase I study of a novel liposomal paclitaxel. *Oncology (Huntingt)* 15, 44–48.
- Vitols, S., Peterson, C., Larsson, O., Holm, P., Aberg, B., 1992. Elevated uptake of low density lipoproteins by human lung cancer tissue in vivo. *Cancer Res.* 52, 6244–6247.
- Walsh, M.T., Atkinson, D., 1990. Calorimetric and spectroscopic investigation of the unfolding of human apolipoprotein B. *J. Lipid Res.* 31, 1051–1062.
- Westesen, K., Gerke, A., Koch, M.H.J., 1995. Characterization of native and drug-loaded human low-density lipoproteins. *J. Pharm. Sci.* 84, 139–147.